

Medical image watermarking based on M-band Wavelet Transform

R. Mavudila¹, Lh. Masmoudi², M. Cherkaoui³,
M. Hamri⁴, N. Hassanain⁵

^{1, 2, 4, 5}(Physics department, LETS Laboratory /Faculty of Science/, Mohammed V University/Morocco)

³(Faculty of medicine and pharmacy/, SIDI Mohammed Ben Abdellah University/CHU CheikZaid/ Morocco)

ABSTRACT: This paper introduces a new reversible and blind scheme based on the analysis of Multi-band Dual Tree Wavelet domain in medical image watermarking domain. Different from many other watermarking schemes with wavelet transform are used on one side in which the studies have dealt only in the dyadic case, in the other hand, in multi-band only on the classical discrete wavelet (DWT), for this suggested approach: security issues for medical information and technical solution to protect these data in medical information are examined. A solution is proposed, which consist in watermarking image areas that are not relevant for the diagnosis, considering advantages of multi-bands wavelet analysis. Applications of the method were examined for MRI images watermarking, inserting data in different sub-bands with private key provides high security for the embedded data using discrete wavelet and complex wavelet (CWT) domain. Experimental results obtained from several watermarked medical images indicate imperceptibility, in each case; the CWT provides higher capacity than the real DWT and DWT domain, by increasing the number of bands. The system is transparent to the user and allows image integrity control; in addition it provides information on the location of potential alterations and evaluation of image modifications which is of major importance in medico-legal frame-work. The proposed method generalizes the findings of previous works.

Keywords: Dual-tree wavelets, medical image, watermarking, multi-band wavelets, watermarking.

I. INTRODUCTION

Medical image protection and authenticity are becoming increasingly important in an e-health era where images are readily distributed over electronic networks. Research has shown that medical image watermarking is a relevant process for enhancing data security, content verification and image fidelity. At the same time, it is necessary to preserve as much original information in the image data as possible, to avoid causing performance loss for human viewers. Most medical image watermarking research focuses on developing watermarking systems that preserve image fidelity and/or robustness, under typical non-medical image degradation processes.

The Digital Imaging and Communications in Medicine (DICOM) standard is the standard to exchange medical data. The DICOM medical image files are attached with header containing patient information which may be lost, attacked or disordered with other header file. However, the watermarking method of medical images using patient information overcomes these problems [1]. However, there is a challenge that interleaving data in a medical image

must not affect the image quality as this may result in wrong diagnosis.

The most promising Dual-Tree wavelet Transform (DTT) proposed by N. Kingsbury, used two classical wavelet trees developed in parallel, looking into the benefits, such as good directional selectivity, shift invariance and perfect signal reconstruction (PR) [2]

The implementation of DT-CWT use couple of filters $\{h_0(n), h_1(n)\}$ to implement one separable wavelet transform and uses another filters couple $\{g_0(n), g_1(n)\}$ to implement [3]. Applying both separable transformations to the some 2D data gives a total of six sub bands: two HL, two LH and two HH subbands.

Being motivated by several applications and advantages of the complex wavelet decomposition in the images processing, we focus our approach by working to put the multi-band extension case to its best directional selectivity and the choice of analysis. This new transform found several applications in image processing, especially that we will exploit in watermarking images [4, 5].

Caroline Chaux proposed the construction of 2D dual-tree M-band wavelet decomposition and suggested that this analysis is the best way in the context of de-noising or higher dimension signal processing [4].

In this paper we presented an extension to M-DT-CWT and, the previously works of Xiangui Kang in [6] and Ning Bi [7] where only the standard DWT have been used.

Taking into account of limitations of DWT, we want to exploit the benefits of DT-CWT by incorporating the principal component analysis (PCA).

Previous work

This paragraph presents, an overview of the important existing watermarking schemes based on wavelet transform in medical domain and other research areas.

We will present them into two cases, dyadic and multi-band cases.

In dyadic case a lots of watermarking schemes are presented in the literature, only with the standard DWT.

Giakoumaki.A and al (2004) proposed a wavelet-based multiple watermarking scheme, which addresses the problems of medical confidentiality protection and both origin and data authentication, this scheme embeds multiple watermarks serving different purposes; a robust watermark for authentication a fragile watermark for the purpose of data integrity control, the scheme added-value tool offers alternatives for different issues associated with medical data management and distribution [8].

Salwa.A. and al(2010) proposed a new method for protecting the patient information in which the information

is embedded as a watermark in the discrete wavelet packet transform (DWPT) of the medical image using the hospital logo as a reference image. The patient information is coded by an error correcting code (ECC), BCH code, to enhance the robustness of the proposed method [9].

Golpina.H andDanyali.H (2009) have proposed a blind reversible watermarking approach for medical images based on histogram shifting in wavelet domain. An integer wavelet transform is applied to map the integer host image components to integer wavelet coefficients. Enabling lossless reconstruction of both watermark and host image, besides providing the high quality for the watermarked image [10].

Cheng-RI and al (2008) proposed a new fragile watermarking algorithm for medical images that makes it possible to resolve the security and forgery problem of the medical images with the discrete wavelet transform, an integer wavelet transform is used to utilize hash function. The watermark associated with the hash values is inserted into the LSBs of the integer wavelet transform coefficients, it can be confirmed that the proposed algorithm detects a forged area of the image very well [11].

ChokriChemak and al(2007) suggested to use the watermarking scheme which preserved the security of medical images for the pocketNeuro project,for reason that image watermarking allows doctors and personnel to hide invisible and robust medical information about a patient [12].

R. Mavudila and al present an algorithm based on dual-tree transform wavelet domain for medical image watermarking, a method that presents a good compromise between robustness and integrity [13]. However only few watermarking methods have been developed willingly the rich properties of dual tree transform wavelet.

With M-band wavelet transform approaches we can observe the works of Ning and al in [7] proposed a blind watermarking scheme based in the multi-band wavelet domain and Empirical mode decomposition.

Xiangui Kang and al, present a new multi-band wavelet scheme by incorporating the principal component analysis (PCA), a blind watermarking technique which achieved higher perceptual transparency and stronger robustness only with the classical Discrete Wavelet Transform (DWT) [6].

We take this latter watermarking embedding strategy in our proposed scheme; particularly we embed watermark bits indirectly in the m-band Dual tree wavelets domain with $M \geq 2$.

II. M-BAND DUAL TREE ANALYSIS (M-DTT)

Given the earlier works of watermarking images based on wavelet transform, we will apply our watermarking by using multi-band ($M \geq 2$ band) in DWT and complex wavelet (CWT) cases, in order to draw good result for a better comparative study.

2.1.Dual-tree Complex Transform (DT-CWT)

The Dual Tree Wavelet Transform initially proposed by N. Kingsburg and further investigated by I. Selesnick, analyses the signal by two DWT trees different with the filters chosen so that at the end of process it returns to approximately the decomposition by analytic wavelet.

The algorithm uses two different sets of filters: h_1 and g_1 , high-pass filters of first and second tree and h_0 and g_0 low-pass first and the second tree. The first tree produces the coefficients of the real part $dr(j,k)$ and the second tree those of the imaginary part $di(j,k)$,we then construct complex coefficients:

$$dcomplex(j,k) = dr(j,k) + i di(j,k). \quad (1)$$

The DT-CWT presents the advantages over simple Hilbert transform of the signal [14].

This implementation uses consists in analyzing the signal by two different DWT trees, with filters chosen so that at the end, the signal returns with the approximate decomposition by an analytical wavelet.

The dual-tree structure has an extension of conjugate filtering in 2-D case.

This structure needs four trees for analysis as well as for synthesis. The pairs of conjugate filters are applied to two dimensions (0 and 1), which can be expressed as:

$$\begin{aligned} (h_0 + jg_0)(h_1 + jg_1) \\ = (h_0h_1 - g_0g_1) + j(h_0g_1 + g_0h_1) \end{aligned} \quad (2)$$

The synthesis of filters suitable for this structure was performed by several people.

The wavelet corresponding to the tree's "imaginary part" is very close to the Hilbert transform of the wavelet corresponding to the trees "real part" [15].

For J level decomposition, the corresponding details sub bands at leven η are denoted: $HL\eta$ real, $HL\eta im$, $LH\eta real$, $LH\eta im$, $HH\eta real$ and $HH\eta im$, where $\eta = 1, 2, \dots, J$.

2.2.M-band Discrete Wavelet Transform (M-DWT).

As reminder that one dimensional dyadic case ($M=2$), is a scaling function $\Phi(x) \in L^2(\mathbb{R})$ and M-1 wavelet function $\{\varphi_l(x), 1 \leq l \leq M-1, M > 2\}$ [16,17] in M-band analysis, these functions satisfy the following equations respectively

$$\Phi(x) = \sum_{k \in \mathbb{Z}} h_1(k) \Phi(Mx - k) \quad (3)$$

$$\varphi_l(x) = \sum_{k \in \mathbb{Z}} h_l(k) \Phi(Mx - k) \quad (4)$$

$$1 \leq l \leq M - 1$$

Where \mathbb{Z} is the integer set and sequence $\{h_l(k), 0 \leq l \leq M-1\}$ has finite length.

The one dimensional Mallat decomposition and reconstruction formulas of orthogonal M-band wavelet are expressed in (5) and (6) respectively [16]

$$C_{j+1} = \sqrt{M} \sum_{k' \in \mathbb{Z}} C_j(k') h_0(k' - Mk) \quad (5)$$

$$d_{j+1} = \sqrt{M} \sum_{k' \in \mathbb{Z}} d_j(k') h_1(k' - Mk)$$

$$1 \leq l \leq M - 1$$

$$C_j(k) = \sqrt{M^{-1}} \sum_{k' \in Z} C_{j+1}(k') h_0(k' - Mk) + \sqrt{M^{-1}} \sum_{l=1}^{M-1} \sum_{k' \in Z} d_{j+1}^l(k) h_1(k' - Mk)$$

$$1 \leq l \leq M - 1 \tag{6}$$

Where $\{C_{j+1}(k), j = 1, 2, \dots, \}$ is the approximation coefficients of the $j+1$ level M -band wavelet decomposition of 1D signal $C_0(k)$ and $\{d_{j+1}^l(k); j = 0, 1, 2, \dots, \}$ is the detail coefficient of the $J+1$ level band wavelets decomposition.

For the image, the 1D M -band discrete wavelet transform is easy to extend to 2D M -band wavelet transform, by applying 1D MDWT

2.3. M-band Dual-Tree (M-DTT)

This implementation uses consisting of analyzing the signal by two different MDWT trees, primal and who gives the real and imaginary coefficients respectively.

The M -band -DT-CWT employs two real M -band DWT.

The first M -DWT gives the real part of the transform while the second MDWT gives the imaginary part.

Let $h_0(n), h_1(n)$ denote the low-pass/high-pass filter and $g_0(n), g_1(n)$ denote the low-pass/high-pass for upper and lower filter banc respectively.

For the scaling function $\Phi^H(x) \in L2(R)$ and $M-1$ wavelet functions $\{\varphi_l^H(x), 1 \leq l \leq M-1, M > 2\}$

The equations (3, 4, 5 and 6) precedents can be used at the primal tree (real part).

In parallel the decomposition applying at dual tree (imaginary part) gives:

$$\Phi^H(x) = \sum_{k \in Z} h_1(k) \Phi^H(Mx - k) \tag{7}$$

$$\varphi_l^H(x) = \sum_{k \in Z} h_1(k) \Phi^H(Mx - k) \tag{8}$$

$$1 \leq l \leq M - 1$$

$$C_{j+1}^H(k) = \sqrt{M} \sum_{k' \in Z} C^H(l) g_0(k' - Mk) \tag{9}$$

$$d_{j+1}^H(k) = \sqrt{M} \sum_{k' \in Z} d_{j+1}^H(k') g_1(k' - Mk)$$

and

$$C_j^H(k) = \sqrt{M^{-1}} \sum_{k' \in Z} C_{j+1}^H(k') g_0(k' - Mk) + \sqrt{M^{-1}} \sum_{l=1}^{M-1} \sum_{k' \in Z} d_{j+1}^H(k) g_1(k' - Mk) \tag{10}$$

Where $\{C_{j+1}^H(k), j = 1, 2, \dots, \}$ are approximation coefficients of the $j+1$ level M -band wavelet decomposition of 1D signal $C^H(k)$ and $\{d_{j+1}^H(k); j = 0, 1, 2\}$ are the detail coefficients of the $J+1$ level band wavelets decomposition.

For the image, the one dimensional DT-CWT M -band can be extended to using the procedure described in section 2 above.

III. WATERMARK EMBEDDING METHOD

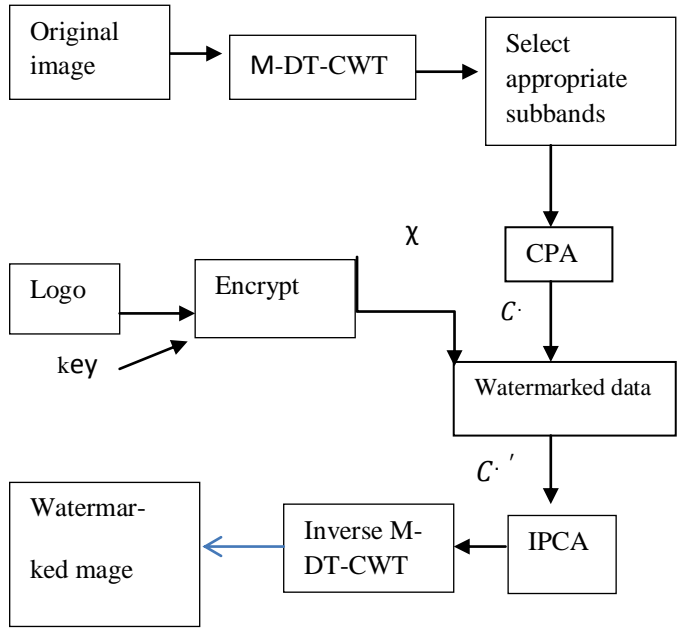


Fig.1. Diagram of embedding watermark

We extend the approach developed in [6], in DT-CWT analyzed an image with DT-CWT equivalent to use two DWT in each tree respectively, in real part and imaginary part.

In this study we will have two components, Primal (real coefficients) and dual (imaginary coefficients).

We consider the watermark logo image Figure 2. encrypted using a 2D pseudo-random sequence with the same size of the logo.

1. The 2D pseudo-random binary (0 and 1) sequence is generated by a key. The binary image logo is XOR operated with the 2D pseudo-random sequence and is raster scanned to obtain a 1D watermark sequence = $\{xi\}, (1 < i < N)$, which is composed of -1 and 1. The occurrence probability of -1 or 1 in X is close to 0.5 because the above encrypting binary sequence is pseudo random sequence (PN).
2. One one level, forward M -band Dual-tree wavelet decomposition is applied to the host medical image $I(x,y)$ we obtain one approximation subband and fifteen detail subbands in each tree (primal and dual) [4,17].
3. Then the coefficients corresponding to the same spatial location in all detail subbands form a one dimensional data array:

$$g_i^1 = (g_i^1.1, g_i^1.2, g_i^1.3, \dots, g_i^1.16) \text{ (Primal tree)}$$

$$g_i^2 = (g_i^2.1, g_i^2.2, g_i^2.3, \dots, g_i^2.16) \text{ (Dual tree)}$$

$1 < i < N$, e.g., a vector of a total of fifteen coefficients, one per subband.

4. The principal component analysis (PCA) is used to transform a coefficient corresponding to the same spatial location in all detail subband [6], it is applied to the obtained ones dimensional matrices are calculated in the tree as follows:

$$V^1 = E(g_i^1 \times g_i^1 T)$$

$$V^2 = E(g_i^2 \times g_i^2 T)$$

where the g_i is the i -th one dimensional data array, E denotes expectation operation and T denotes the matrix transpose operation.

-The eigenvectors Φ (basis function) corresponding to eigenvalue ζ of the covariance matrix respectively:

$$V^1 \cdot V^1 \zeta \Phi^1 \text{ and } V^2 \cdot V^2 \zeta \Phi^2$$

Where eigenvectors Φ are sorted in descending order:

$$\Phi^1 = (\varphi_1^1, \varphi_2^1, \varphi_3^1, \dots, \varphi_{16}^1)$$

$$\Phi^2 = (\varphi_1^2, \varphi_2^2, \varphi_3^2, \dots, \varphi_{16}^2)$$

-Then calculate the PCA components;

$$p^1 i = \Phi^1 T g^1 i = (p^1 i.1, p^1 i.2, p^1 i.3, \dots, p^1 i.16)$$

(Primal tree)

$$p^2 i = \Phi^2 T g^2 i = (p^2 i.1, p^2 i.2, p^2 i.3, \dots, p^2 i.16)$$

(Dual tree).

In the following, we can write the data with $(.)$ to indicate 1 or 2 for defined the real and imaginary parts respectively (e.g. $C \cdot$ instead of C^1 or C^2).

4. All the obtained first principle components $p \cdot i.1$ ($1 < i < N$) from a 1-D array $\{C \cdot \{C \cdot (i)\} | C \cdot (i) = \{p \cdot i.1, 1 < i < N\}$ in the same raster scanning fashion as in step:

1. Finally, watermark X is embedded in the principle components $C \cdot$ using quantization-based method [18,19,20] equation (11) to obtain $C \cdot'$, where $C \cdot (i)$ and $C \cdot' (i)$ denote the i -th element in $C \cdot$ and $C \cdot'$, respectively. The quantizer $q(\cdot)$ is a uniform, scalar quantization function of step size S , and $q(x) = kS + 0.5S$,

$$k = x \left\lfloor \frac{x}{S} \right\rfloor \quad (k \in Z)$$

Where $\lfloor \cdot \rfloor$ denotes the floor operation.

The embedding strength S can be chosen so as, to achieve a good compromise between the contending requirements of imperceptibility and robustness. Note that the difference between $C \cdot (i)$ and $C \cdot' (i)$ is between $-0.5S$ and $+0.5S$.

If $x = -1$, $C \cdot (i) \bmod S = 0.25S$. If $x_i = +1$, $C \cdot (i) \bmod S = 0.75S$.

Where \bmod denotes the signed remainder after division.

5. Apply inverse PCA on the modified PCA components to obtain the modified one dimensional wavelet coefficients array.

6. Performing inverse M-band DT-CWT on the modified image coefficients, we obtain a watermarked image $\Gamma'(x, y)$.

$$\begin{cases} C \cdot' (i) = g \left(C \cdot (i) - \frac{1}{4S} \right) + \frac{1}{4S}, & \text{if } x_i = 1 \\ C \cdot' (i) = g \left(C \cdot (i) + \frac{1}{4S} \right) - \frac{1}{4S}, & \text{if } x_i = -1 \end{cases} \quad (11)$$

$$x_i^* = \begin{cases} +1, & r = C \cdot^*(i) \bmod S > S/2 \\ -1, & \text{otherwise} \end{cases} \quad (12)$$

Watermark detection

The watermark extraction is the inverse process of watermark embedding. The test image is M DT-CWT decomposed, then PCA is applied, and the first principle components are obtained to form a 1-D array $C \cdot^* \{C \cdot^* (i), (1 < i < N)\}$. $C \cdot^* (i)$ is the extracted principle component. According to equation (12), we can extract the hidden binary data $X^* \{x \cdot^* (i), (1 < i < N)\}$.

Equation (12) indicates that if $r (r = C \cdot^*(i) \bmod S)$ is in the interval $(0, 0.5S)$, then the decision is made in favor of " $x_i^* = -1$ ". Otherwise, " $x_i^* = 1$ ". Then following correlation coefficient is used to decide if the watermark exists in the test image

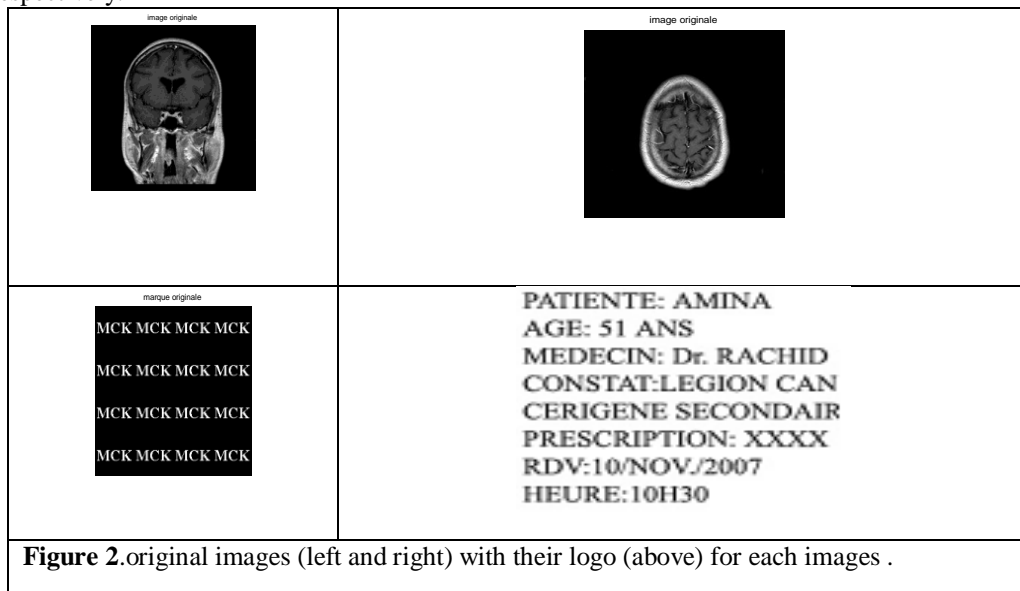
$$p_{x, x^*} = \frac{x \cdot x^*}{\|X\|} \quad (14)$$

where $\|X\|$ is the size of the watermark X (that is N in this paper) and $X \cdot X^*$ is the inner product of X and the extracted sequence X^* .

If the correlation coefficient between the embedded sequence X and the extracted sequence X^* from a test image is larger than a threshold (δ) , i.e. $p_{x, x^*} \geq \delta$, we can determine that watermark exists and we write "1", or "0" if no [21].

IV. Results and Discussion

The proposed approach has been tested for two MRI images of the size 250x250 shown in 'Fig.2', with their logo images (watermark) respectively.



The data obtained, shows that 3-band leads to visually better results and the details are well explained in ‘Fig.3 and 4’, compared to the case of 2-band.

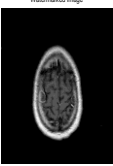
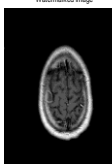
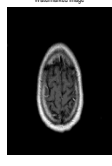
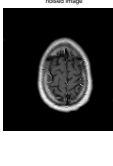
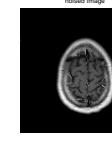
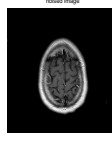
If we exploit only a process for dyadic case the best results are for CWT following real DWT see the benefits of DT-CWT and advantages of M-band in statically characteristic processing in noise study, mentioned previously [4]. For each transformed DWT or DT-CWT, the result is improving as and when we increase the number of bands.

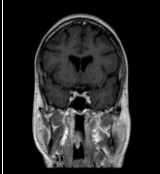
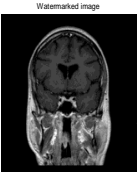
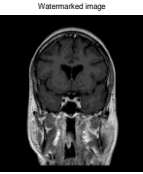
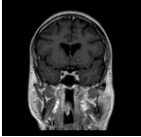
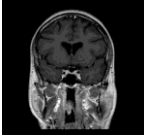
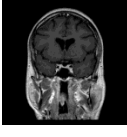
‘Fig.3 and 4’, shows the results after applying DWT and DT-CWT in 2-band and 3-band to the MRI images respectively, we only used the one- resolution level.

Analysis of the results shows that the proposed scheme has high degree of robustness to each attack in $M > 2$ bands. For Gaussian noise attack, the presence of watermark is ‘0’ with the variance > 0.005 in axial images in both cases.

We have tested the proposed algorithm on many attacks. The watermark is robust to JPEG compression with quality factor as low as 15% (JPEG 15) and to common image processing such as median filtering Gaussian filtering. The watermark could be detected when the marked image has been cropped by 50%. We compare the proposed algorithm M-DT-CWT watermarking with DWT dyadic case, for fair comparison, in DWT.

I. FIGURES AND TABLES

M	DWT	realDWT	CWT
2			
	a.(PSNR :37.2)	b.(PSNR :39.1)	c.(PSNR :40.2)
3			
	d.(PSNR :39.3)	e.(PSNR :40.1)	f.(PSNR :42.0)
Figure 3 : a , d. watermarked images without attack (DWT left), b , e. (real DWT middle) and c , f (CWT right)			

M	DWT	realDWT	CWT
2			
	PSNR:39.01	PSNR:40.12	PSNR:41.19
3			
	PSNR:40.15	PSNR:41.15	PSNR:42.48
Figure 4: a, d. watermarked images without attack (DWT left), b,e (real DWT middle) and c,f (CWT. left)			

The performance and robustness have been tested with the attacks of image processing the presence the watermark in the attacked images shown in “Table2”above. PSNRs results (in dB) of the watermarked image after attacks are shown in table 1, we find the performances for M=3 band in comparison with M=2 band, also those of CWT to DWT for each case.

Table 1: PSNR VALUE BETWEEN ORIGINAL IMAGES AND WATERMARKED IMAGES

Band number	PSNR (Coronal image)		PSNR (Axial image)		
	DWT	CWT	DWT	CWT	Attacks
M = 2	30.23	35.33	30.12	35.10	JPEG 15%
M = 3	33.62	36.10	33.29	36.01	
M = 2	30.12	32.53	30.01	32.10	Rotation 10°
M = 3	31.45	32.98	30.25	33.29	
M = 2	30.43	32.25	29.45	30.05	Median filter (3x3)
M = 3	32.44	33.55	30.45	33.55	
M = 2	26.95	28.67	25.51	29.07	Cropping 50%
M = 3	30.11	32.20	30.10	31.45	
M=2	29.21	30.23	28.45	29.74	Sharpen attack
M=3	30.12	31.10	30.25	32.19	

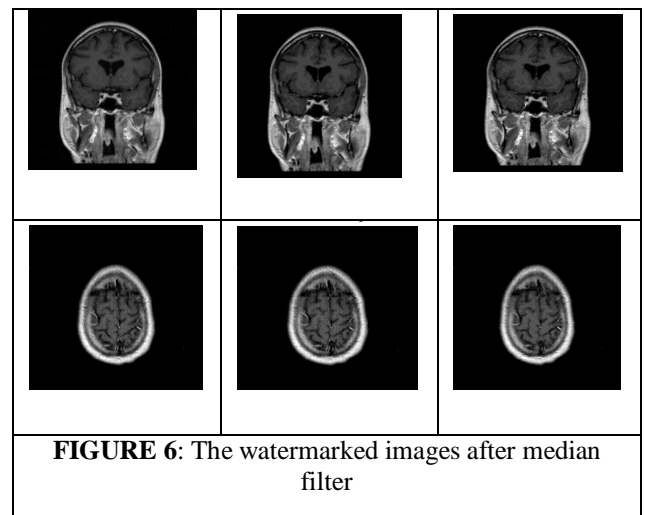
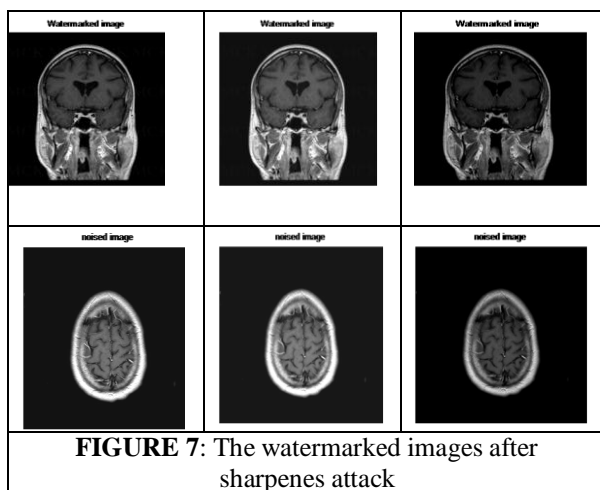
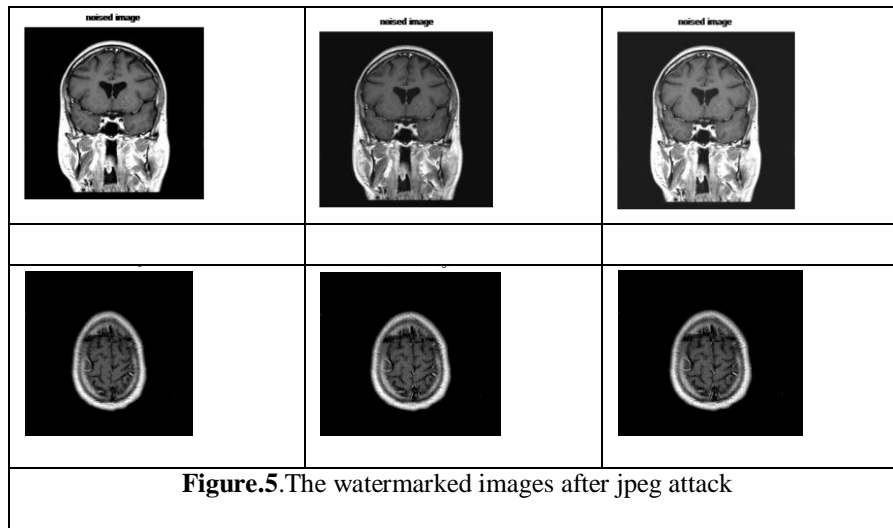
“Table2”, show the robustness of our approach to the attacks, the results are visually impressive, better for the case M = 3 bands, and also for the M-band analysis. The watermarked images obtained are shown in “Fig. 2.”

Table 2: THE PRESENCE OF WATERMARK IN THE STEP OF DETECTION.

Band	presence in Coronal image		presence in Axial image		
	DWT	CWT	DWT	CWT	Attacks
2	0	1	0	1	JPEG 15%
3	1	1	1	1	
2	0	1	0	1	Rotation 10°
3	1	1	1	1	
2	0	1	0	1	Median filter(3x3)
3	0	1	1	1	
2	0	1	0	0	Cropping 50%
3	1	1	1	1	
2	0	1	0	1	Sharpen attack
3	1	1	1	1	

The obtained PSNR values with M-DWT for M=2 bands and M=3 bands are presented” in Table 1”, respectively; while the marked image in M-DT-CWT domain, with 3-band has excellent perceptual quality without any artifacts.

‘‘In Fig.5,6 and 7’’, are shown the result of the watermarked images after common attacks onlyfor M =3 case.



Robustness of the scheme is so proved against JPEG, with different quality factors (QF<60%) for the two images in DT-CWT and $M > 2$ band, the presence of watermark.is successfully recovered.

In Axial cropped image by 50° , the presence of watermark is no found in each wavelet analysis case.

The medical images have some diversity and their treatment may differ from case to case. Clinical information then locates areas that define and separate Regions of Interest (ROI) we seek to highlight the anatomical and pathological structures that detected by physicians sought after diagnosis.

By ttaking into account the specificity of these images, we manage these ROI, for the watermarking. Therresults made object of blind test of more than technicians and doctors of the hospitals who affirmed that for images shown in ‘Fig.3and 4’’, had a good perceptually visibility after watermarking.

In addition for the test result, it shows the following observation; All images were considered acceptable for diagnosis by all observers for all Multi-band of DT-CWT and suggested that the images DWT are degraded to be retable with the geometric attack in dyadic case. Finally overall test result support the previous confirmations in all cases

V. CONCLUSION

The performances of the complex wavelet transform for watermarking image in dyadic cases are already demonstrated in the literature. In our work, efforts are to generalize their conclusions by demonstrating the efficiency of the complex multi-band wavelet transform, in consideration of its qualities. It can be concluded that the implementation of M-band complex wavelet can be treated as the best for watermarking images by considering the results of watermarked image summarized in the figures. The additional privilege of the suggested algorithm is its compatibility with human visual characteristics to embed the watermark for a high number of bands. In this way higher capacity of M-band wavelet domain is applied to embed the watermark information along with preserving the quality and clinical information of medical images and integrity of watermarked image which is of major importance in medico-legal frame work.

In future we open the way for researchers for the detection step which shows how to extract the watermark in integrality.

Acknowledgements

The authors are grateful to physicians and medical technique staff in a medical images service centre at CheikZaid hospital (Morocco) for their entire assistance and suggestions during data collection in test step. The special thanks to Caroline Chaux ,Xiangui Kang and al for their contributions in Multi-band wavelets domain ,source of inspirations in this work.

REFERENCES

- [1] Colín R, Uribe C F, and Villanueva J A M. 'Robust watermarking scheme applied to radiological medical images'. *IEICE Trans. Inf. Syst.* E91-D(3):862–864,2008.
- [2] N.G.Kingsbury.'The dual-tree complex wavelet transform: 'A new technique for shift invariance and directional filter'. *In proc.IEE Digital Signal Processing Workshop*, n°86, Bryce canyon, UT,USA, Aug.9-12, 1998.
- [3] P.Loo and NG.Kingsbury.' Digital watermarking using complex wavelets', *proc.ICIP 2000,Vancouver ,sep.2000.*
- [4] Caroline Chaux, Laurent Duval et Jean-Christophe P. 'Image Analysis Using a Dual-Tree M-Band Wavelet Transform'. *IEEE Transactions on Image Processing*, Vol.15, No. 8, p. 2397-2412, août 2006.
- [5] Caroline C. 'Analyse M-bandes en arbre dual, application à la restauration d'images', thèse , Université de Marne la vallée, 2006.
- [6] Xiangui K, Wenjun Zeng and Jiwu Huang . 'A Multi-band Wavelet Watermarking Scheme'. *International Journal of Network Security*, Vol.6, No.2, PP.121–126,Mar.2008 ,
- [7] Ning Bi, Qiyu Sun, D. Huang and al, 'Robust Image Watermarking Based on Multi-band Wavelets and Empirical mode Decomposition', *IEEE Trans. On Image Proc.*, vol. 16, n°8, August 2007
- [8] Giakoumaki, A. Paulopoulos and al, 'A Medical image watermarking scheme based on wavelet transform'. *In Engineering in Medicine and biology society*, 2003
- [9] Salwa A.K, Naser el-Sheiny and al. Wavelet packets-based blind watermarking of medical image management. *Open Bio Med Eng.* J.2010; 4: 93-98.
- [10] Golpira H, Danyali H. 'A blind reversible watermarking based on histogram shifting for medical image'. *Signal processing and information Technology (ISSPIT)*, 2009, *IEEE*.
- [11] Chen-Ri Piao, Dond-Min and al. 'Medical Image Authentication Using hash Function and Integer wavelet Transform'. *Image and Signal processing, congress 2008*, on vol.1, pp 7-10
- [12] Chokri C and al. 'New watermarking Scheme for security and transmission of medical images for packet Neuro project'. *Radio Engineering*, vol.4, Dec.2007.
- [13] Mavudila R, Masmoudi L and al. 'Transformée en ondelette en arbre-dual pour le tatouage d'images médicales'. *Revue Congolaise des Sciences Nucléaires*, vol.24, p.184-198 ; Décembre 2010.
- [14] Selesnick I, Baraniuk I.R.G and N.G.Kingsbury N. 'The dual-tree complex wavelet transform'. *IEE Signal Processing magazine*, vol.22, n°6, pp.123-151, nov.2005.
- [15] Selesnick I and K.Li. 'Video denoising using 2D and 3D dual-tree complex wavelet transforms'. *in wavelet applications in signal and image processing X (proc.SPIE 5207)* 2003.
- [16] N. Bi, D. Huang, Q. Dai and al, 'A class of orthogonal and symmetric 4-band wavelets with one parameter'. *Mathematical Numerical Sinica*, vol.27, n°2, 11-10, Mai 2005.
- [17] Q.Sun, N.Bi, D., Huang, 'An Introduction to Multi-band Wavelets', *Zhejiang University press*, 2001.
- [18] B. Chen and G. W. Wornell, "Quantization index modulation: A class of provably good methods for digital watermarking and information embedding," *IEEE Transactions on Information Theory*, vol. 47, no. 4, pp. 1423-1443, May 2001
- [19] X. Kang, J. Huang, Y. Q. Shi, and Y. Lin, "ADWT-DFT composite watermarking scheme robust to both affine transform and JPEG compression," *IEEE Transactions on Circuits and Systems for Video Technology*, vol.13, no. [8], pp. 776-786, Aug. 2003
- [20] M. Wu, and B. Liu, "Data hiding in images and video: Part I: fundamental issues and solutions," *IEEE Transactions on Image Processing*, vol. 12, no. 6, pp. 685-695, Jun. 2003.
- [21] I. Cox, J. Kilian, T. Leighton, and T. Shamon, "Secure spread spectrum watermarking for multimedia," *IEEE Transactions on Image Processing*, vol. 6, no. 12, pp. 1673-1687, 1997.